UCRL-JC-124878
PREPRINT

Laser-Induced Damage of Fused Silica at 355 and 1064 nm Initiated at Aluminum Contamination Particles on the Surface

**F. Y. Génin, K. Michlitsch, J. Furr,
M. R. Kozlowski, and P. Krulevitch**

**This paper was prepared for submittal to the
28th Annual Symposium on Optical Materials
for High Power Lasers
Boulder, Colorado
October 7-9, 1996**

January 24, 1997

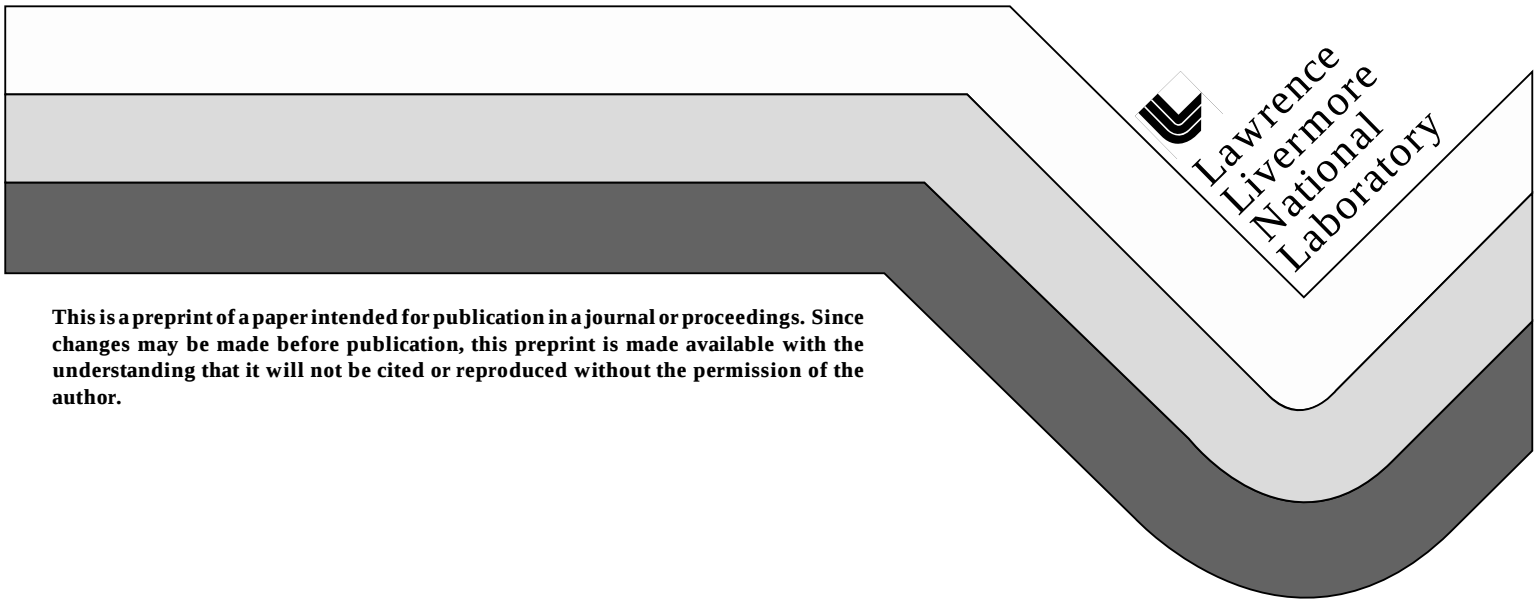

Laser-induced damage of fused silica at 355 and 1064 nm initiated at aluminum contamination particles on the surface

F. Y. Génin[a)], K. Michlitsch, J. Furr, M. R. Kozlowski, and P. Krulevitch

Lawrence Livermore National Laboratory,
Laser Materials Department, Livermore, California 94550

ABSTRACT

Contamination particles of controlled size and shape were deposited onto 1.14 cm thick fused silica windows by sputtering Al through a mask. The particles were 1 µm thick circular dots, 10 to 250 µm in diameter. Al shavings were also deposited on the windows to investigate the effects of particle-substrate adhesion. The silica windows were then illuminated repetitively using a 3-ns, 355 nm and an 8.6-ns, 1064 nm laser. The tests were conducted at near normal incidence with particles on the input and output surfaces of the window.

During the first shot, a plasma ignited at the metal particle and damage initiated on the fused silica surface. The morphological features of the damage initiated at the metal dots were very reproducible but different for input and output surface contamination. For input surface contamination, minor damage occurred where the particle was located; such damage ceased to grow with the removal of contaminant material. More serious damage (pits and cracks) was initiated on the output surface (especially at 355 nm) and grew to catastrophic proportions after few shots. Output surface contaminants were usually ejected on the initial shot, leaving a wave pattern on the surface. No further damage occurred with subsequent shots unless a shot (usually the first shot) cracked the surface; such behavior was mostly observed at 355 nm and occasionally for large shavings at 1064 nm.

The size of the damaged area scaled with the size of the particle (except when catastrophic damage occurred). The onset of catastrophic damage on the output surface occurred only when particles exceeded a critical size. The damage behavior of the sputtered dots was found to be qualitatively similar to that of the shavings. The artificial contamination technique accelerated the study by allowing better control of the test conditions.

Keywords: Surface contamination, laser-induced damage, functional damage, damage morphology, fused silica, metal contamination, 355 nm, 1064 nm.

1. INTRODUCTION

The development and application of high fluence laser for inertial confinement fusion such as the National Ignition Facility (NIF) at Lawrence Livermore National Laboratory (LLNL) or the Laser Mégajoule (LMJ) in France continues to generate strong interest in the behavior of optical components under intense illumination. These solid state lasers create a very harsh environment as designers push the fluence levels closer and closer to the damage thresholds of the optics. Optics can be damaged by the laser beam as a result of the limitations inherent to the bulk or surface properties. Contamination particles on the surface can aggravate this damage. The effect of contaminants on the onset of damage must be characterized and quantified in order to predict the survivability of optics on the beam line and set cleanliness requirements which can prevent or delay damage.

[a)] Electronic Mail: fgenin@llnl.gov

While contamination effects are known to degrade the damage thresholds of optical components,[1-13] very little has been done to quantify these effects. Optics development efforts have mainly focused on improving their intrinsic properties or reducing imperfections in optical materials.[14-16] The study presented in this article was designed to quantify the effects of surface contamination particles on the functional damage threshold of NIF optics. The initial matrix of variables to be investigated included contamination material (e.g. metals, oxides, organics), particle size, shape and mass, substrate material (e.g. fused silica, phosphate glass, KDP, multilayer mirrors and polarizers), wavelength, environment (air, vacuum), fluence level and number of shots.

This article will only present the results of 1-on-1 (single shot), N-on-1 (N successive shots) and S-on-1 (600 shots at a 10 Hz repetition rate) tests for Al contamination on fused silica surfaces at 1064 and 355 nm. The study was performed for contamination on both input and output surfaces of the silica window. In order to control the size and shape of the contamination particles, 1 μm thick Al dots of sizes ranging from 10 μm to 250 μm were sputter-deposited onto the silica; the 250 μm maximum contamination size was chosen since calculations showed that obscurations larger than 280 μm would not be tolerable (because of potential down-stream propagation)[17] but the effect of smaller particles on laser-induced damage was not known. Pure Al shavings deposited onto the silica were also irradiated. The results proved to be very reproducible and showed that the behavior of dots and shavings are qualitatively very similar.

The discussion in this article mainly concentrates on the damage morphologies. Damage was classified into three categories: benign, massive and catastrophic (also referred to as massive unstable). Catastrophic damage can be described as glass cracking or being ablated during repetitive illumination. Massive damage refers to damage which will affect the performance of the optic beyond NIF tolerance limits (e.g. damage larger than 280 μm). Benign damage does not compromise the laser performance. The damage morphologies were found to be very consistent for Al particles of different sizes but changed for contamination on the input versus output surface.

Since damage was more severe at 355 nm than 1064 nm, this article describes the dependence between damage size and contamination size for massive damage at 1064 nm while it focuses on the relationship between contamination size and fluence levels inducing catastrophic damage at 355 nm.

2. EXPERIMENTAL PROCEDURE

2.1 Preparation of contaminated optics

Low stress CVD silicon nitride was deposited onto 3” silicon wafers. Small holes were etched into the nitride on the front side using standard photolithography techniques and larger squares were etched on the back. The wafers were then dipped several hours in a bath of KOH at 70°C to anisotropically etch the silicon and open the windows. Six different circle sizes were etched: 10, 20, 30, 50, 150 μm and 250 μm. The masks were placed onto 1.14 cm thick Corning 7980 Zygo superpolished fused silica substrates. Aluminum was then sputter-deposited until the thickness of the deposit reached 1 μm. All the substrates were subjected to a standard cleaning procedure prior to the deposition of Al.

For the Al shavings tests, the samples were contaminated by breathing on the substrate for adhesion and then filing high purity Al over the substrate. An initial study determined that the Al shavings adhered well enough to remain on the substrate during the laser tests.

2.2 Laser testing conditions

The testing proceeded as follows:

- laser damage testing of the thin metal dots on the substrates at 1064 nm or 355 nm,
- characterization of the laser-induced damage after the 1-on-1, 20-on-1, and S-on-1 tests by Nomarski optical microscopy and measurements of the damage size. The tests were interrupted as soon as catastrophic damage initiated.

The damage threshold of the surface of the fused silica samples was first tested to establish a baseline; the threshold (scaled to a 3-ns pulse length) of the uncontaminated surface was above 50 J/cm^2 at 1064 nm and 15 J/cm^2 at 355 nm. The damage threshold standard deviation of the clean fused silica was about 1.5 J/cm^2.

The laser damage tests were carried out using a 3-ns and 8.6-ns pulse from a 355 nm and 1064 nm Nd:YAG laser, respectively.[18] The laser was focused to provide a far field circular Gaussian beam with a diameter of about 1 mm at 1/e^2 of the maximum intensity. The beam profile was recorded for each shot (except for the S-on-1 tests) and the peak fluence was computed. The tests were conducted in s-polarization at 1° and 5° incidence angle for the 355 nm and 1064 nm laser, respectively. Fluences during tests were 20 and 40 J/cm^2 at 1064 nm and between 1 and 17 J/cm^2 at 355 nm.

In order to obtain sufficient statistical information at 1064 nm, 5 dots of a given size were tested. Six particle sizes were investigated (10, 20, 30, 50, 150, and 250 µm). The damage morphology was characterized after the 1-on-1, 20-on-1 and S-on-1 tests by Nomarski and back light optical microscopy in order to measure the size of the damage.

A set of shavings were illuminated 1-on-1, 20-on-1 and S-on-1 on both input and output surfaces at 20 and 40 J/cm^2. The study was determined feasible, although much more difficult, time consuming and less standardized than for the sputtered Al dots.

3. RESULTS AT 1064 NM

This section first presents the input surface and output surface sputtered dots results and second the tests with the shavings. The tests provided very reproducible damage morphologies (see Figs. 1 and 2). The damage behavior (i.e. size and morphology) was found to be different when the contaminant is on the input surface as opposed to the output surface. The behavior of the shavings deposited on silica was found to be qualitatively similar to that of the sputtered particles, even though the adhesion properties are significantly different.

3.1 Input surface sputtered Al contaminant:

Damage can initiate on the silica surface at and around the metal dot. During the first pulse, a plasma ignites at the dot, Al is molten or evaporated and can re-deposit in the surroundings. Each subsequent pulse can then interact with the fresh deposit until it no longer ignites a plasma. Damage is then stable. The surface morphology is that of a burnt surface with a large number of small craters. The morphologies of damage after 1, 20, and 600 shots are shown in Fig. 1. Figure 3 shows the damage size as a function of initial dot size. The larger the dot, the more material is re-deposited in the immediate vicinity and the larger the size of damage. For particles in the 0 to 300 µm size range, if the damage is benign or massive, its size will reach on average about 2.9 times the size of the initial contamination.

On-going work is being performed to quantify the effect of damage on the characteristics of the transmitted beam (phase shifts, loss of transmitivity) in order to refine the measurements of the damage size. The phase shifts are measured by interference microscopy.

3.2 Output surface sputtered Al contaminant:

For output surface contamination, damage only occurs at the metal particle. A plasma ignites at the metal on the first shot. Usually, subsequent shots do not produce plasmas and no further damage on the surface occurs. The pulse often leaves a fine wave pattern at and in the vicinity of the metal. Figure 2 shows the typical morphologies for the six dot sizes. Figure 4 plots damage size as a function of contamination size. In the 0 to 300 µm particle size range, if the damage is not catastrophic, on average, its size will reach about 1.4 times the size of the initial contamination.

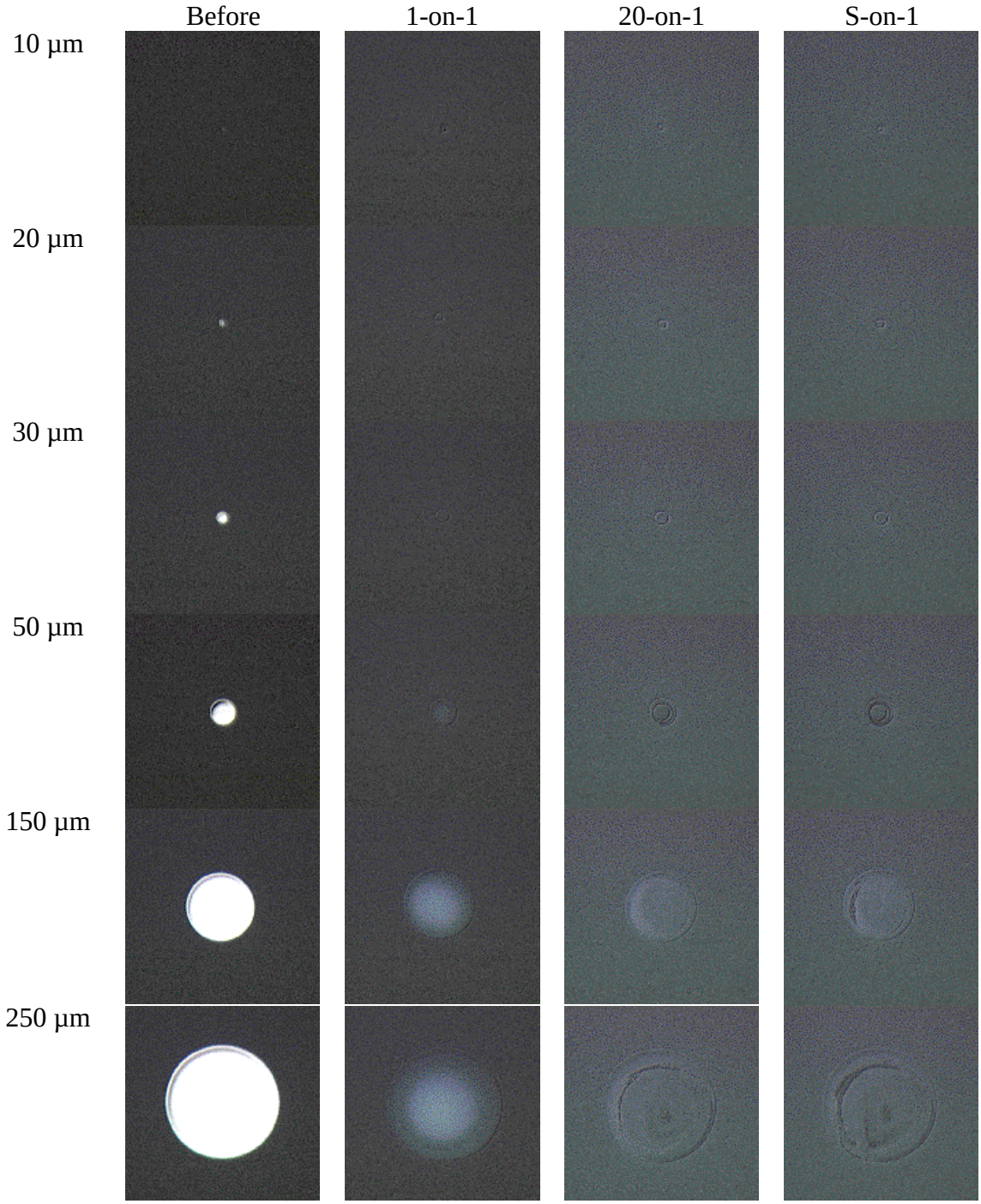

Fig. 1: Nomarski optical micrograph of the typical damage morphology of the input surface of the fused silica window after 1-on-1, 20-on-1 and S-on-1 tests on the 10, 20, 30, 50, 150 and 250 µm sputtered 1 µm thick aluminum dots, at 1064 nm and 40 J/cm^2. The dots are located on the *input surface*.

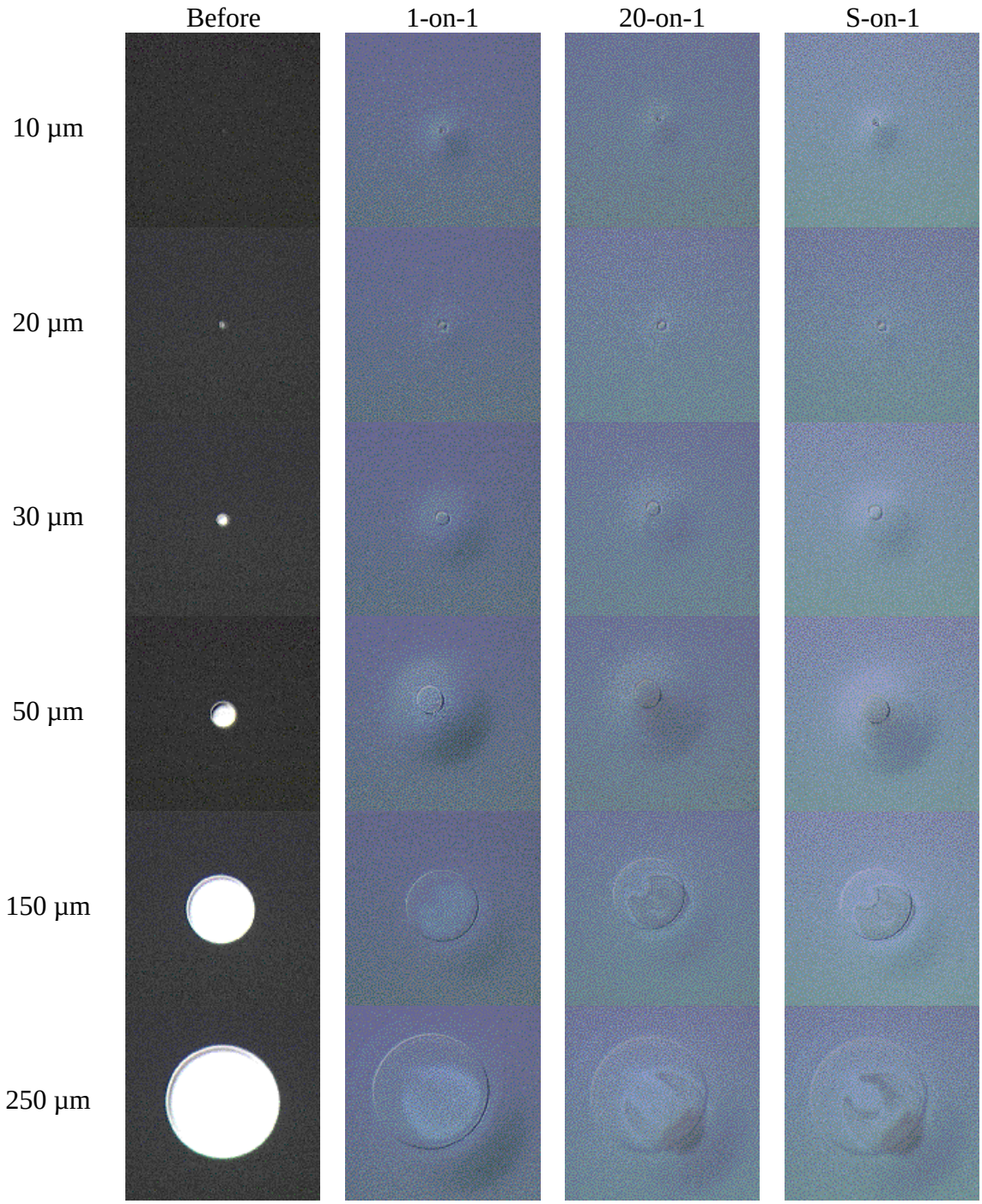

Fig. 2: Nomarski optical micrograph of the typical damage morphology of the output surface of the fused silica window after 1-on-1, 20-on-1 and S-on-1 tests on the 10, 20, 30, 50, 150 and 250 µm sputtered 1 µm thick aluminum dots, at 1064 nm and 40 J/cm^2. The dots are located on the *output surface*.

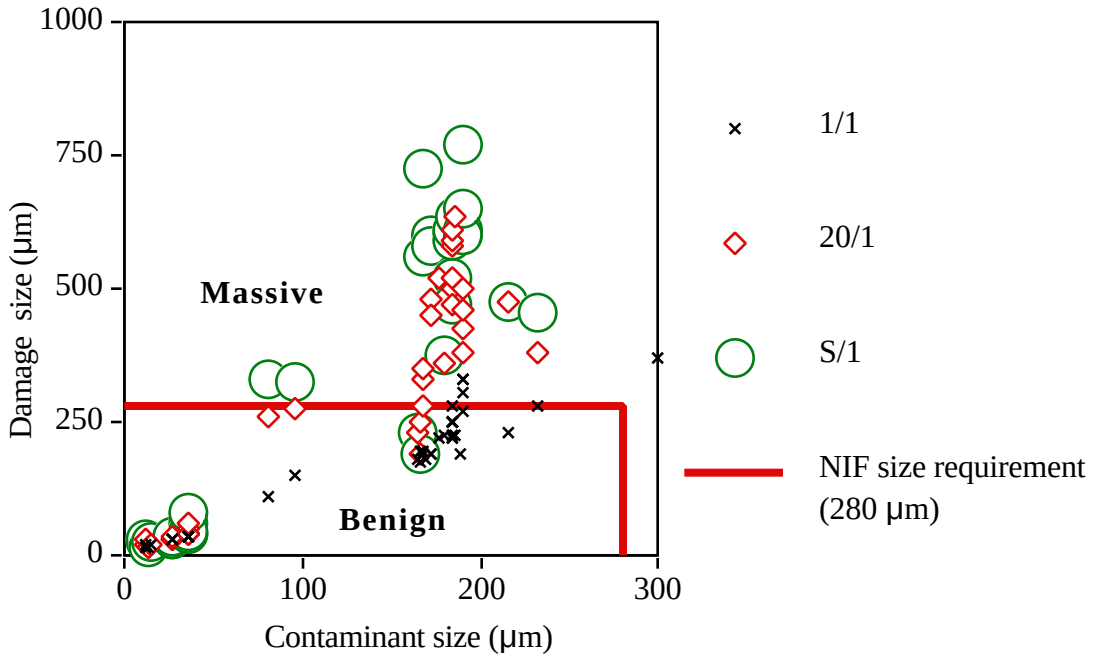

Fig. 3: Input surface damage size as a function of *input surface* contaminant size for 1 μm thick sputtered Al dots after 1-on-1, 20-on-1 and S-on-1 tests at 1064 nm and 40 J/cm^2. Input surface damage can grow with subsequent shots, but quickly reaches an asymptotic size. No output surface damage was detected during this series of tests.

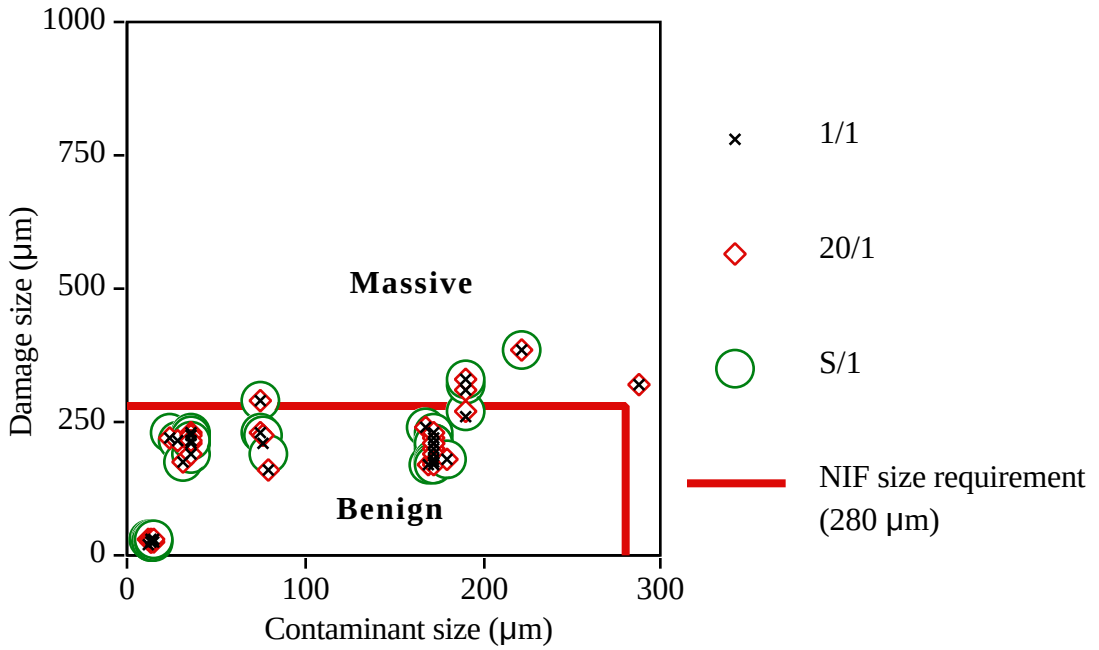

Fig. 4: Output surface damage size as a function of *output surface* contaminant size for 1 μm thick sputtered Al dots after 1-on-1, 20-on-1 and S-on-1 tests at 1064 nm and 40 J/cm^2. The damage did not grow with subsequent shots (no catastrophic damage) for thin series of thin particles.

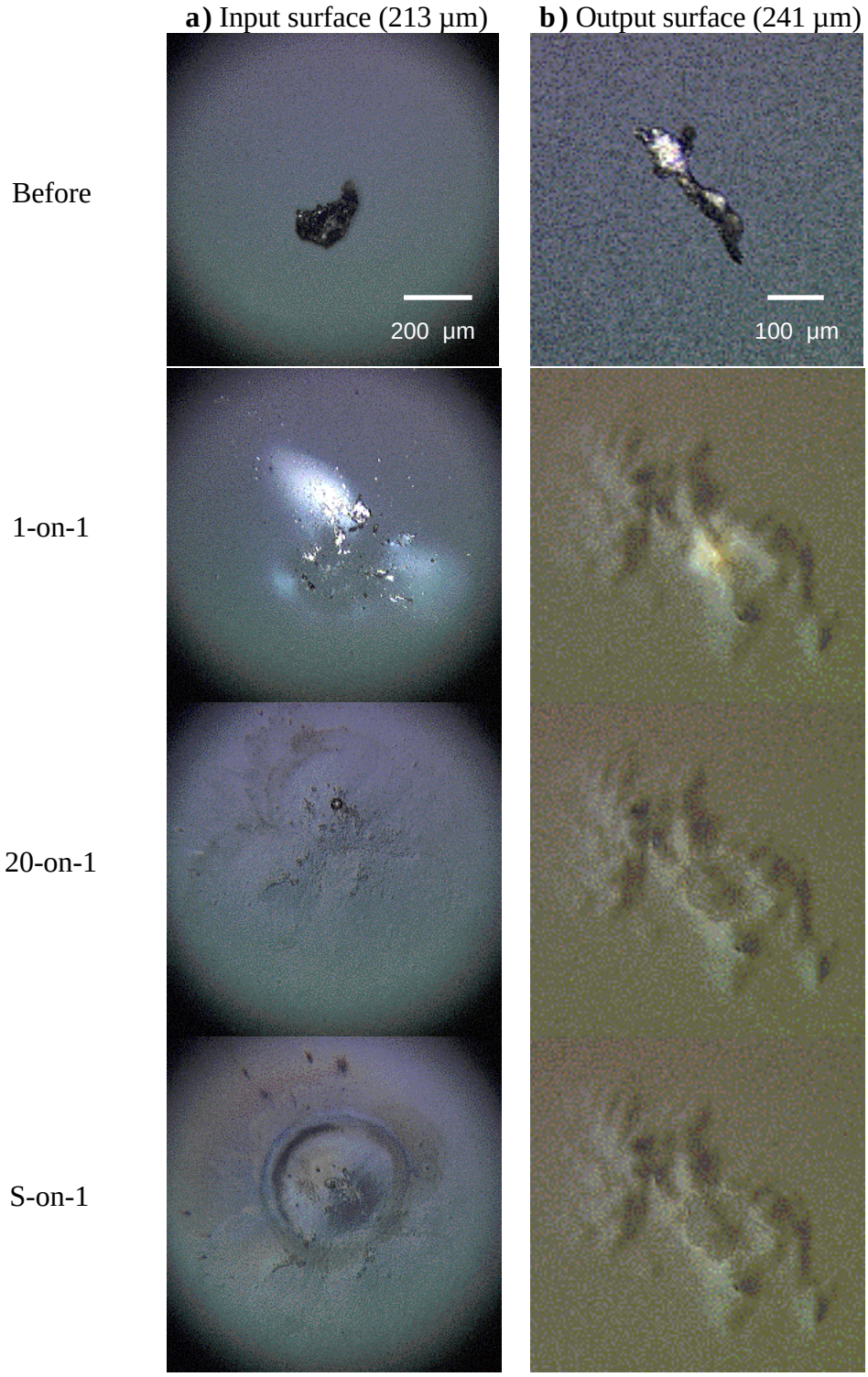

Fig. 5: Nomarski optical micrograph of the typical damage morphology initiated by aluminum shavings located on a) the input and b) the output surface of the fused silica window after 1-on-1, 20-on-1 and S-on-1 tests at 1064 nm and 40 J/cm^2.

3.3 Al shavings:

The damage morphologies initiated at Al shavings are consistent with those observed for sputtered dots (see Fig. 5). Some differences are expected as a result of the difference in mass and shape of the particle.

Input surface damage consists of bumps in the center region, craters surrounding, and debris scattered farther away. During the first shot, the laser energy is partially absorbed by the contaminant. This vaporizes the Al and leaves an Al deposit on the surface. Such a deposit behaves like the sputtered dots upon subsequent illumination.

Damage from output surface contaminants exhibits the characteristic rear surface wave pattern (see Fig. 5) and usually grows very little after the first shot; the Al shaving is usually blown off on the first shot. Cracks were initiated in a few cases on the first shot on large particles. Such damage grew very quickly to catastrophic proportions (see Fig. 6). The pit initiated on the output surface and subsequent shots drilled into the bulk of the glass by coupling with the light. This phenomenon occurs when the first shot is able to produce cracks in the silica. Since catastrophic failure did not occur for the 1 μm thick sputtered dots, it is believed that the higher particle mass leads to larger momentum transfer to the glass during the pulse. The plots of damage size vs. contamination size for both input and output surface contamination are shown in Figs. 7 and 8. The damage morphology of the shavings is similar to that of the sputtered dots, but the damage size is generally larger (probably due to the larger mass of the shavings).

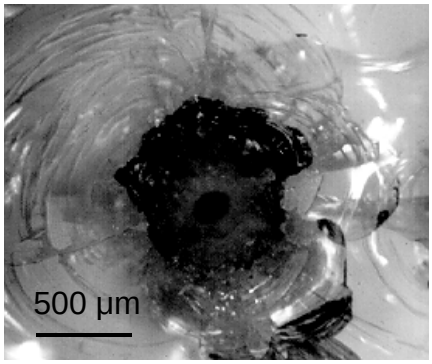

Fig. 6: Nomarski optical micrograph of the catastrophic damage morphology at 1064 nm of the output surface cracks of the fused silica window after several shots at 40 J/cm^2. An aluminum shaving was located on the output surface. If cracking occurs, the output surface is easily drilled by the laser beam. Such damage rarely initiates at 40 J/cm^2 at 1064 nm for aluminum. However, at 355 nm, it is much more common and can be triggered by both input and output surface contamination.

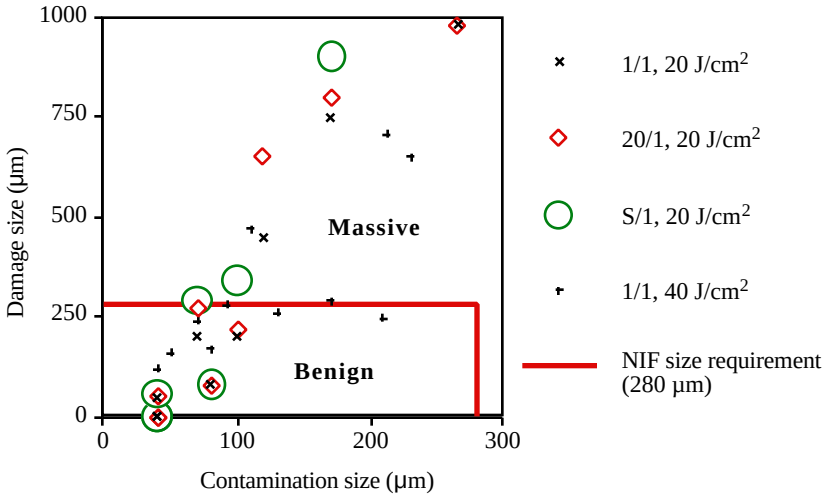

Fig. 7: Input surface damage size as a function of *input surface* contaminant size for Al shavings after 1-on-1 tests at 40 J/cm^2, and 1-on-1, 20-on-1 and S-on-1 tests at 20 J/cm^2 and for 1064 nm wavelength. No output surface damage was detected during this series of tests.

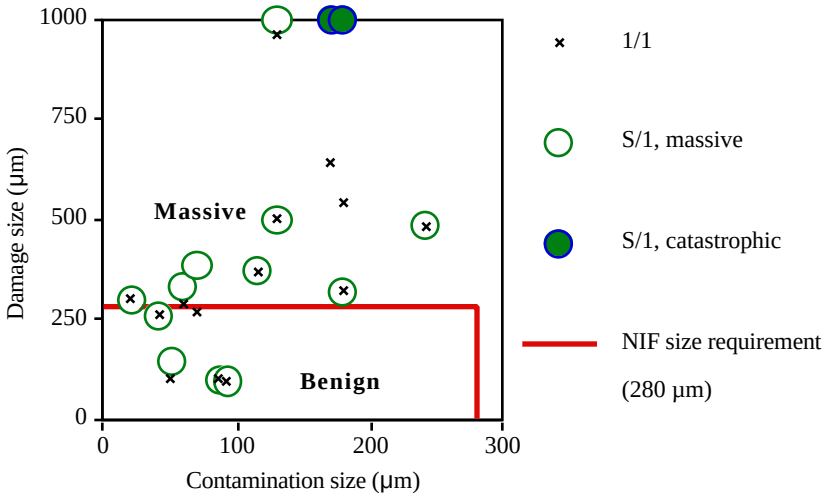

Fig. 8: Output surface damage size as a function of *output surface* contaminant size for Al shavings after 1-on-1 and S-on-1 tests at 1064 nm and 40 J/cm^2. This damage does not grow with subsequent shots for the smaller particles. Since catastrophic damage occurred twice during the shaving tests and not for the thin sputtered deposited dots. It is believed that the mass of the particle plays an important role in initiating a crack in the fused silica.

4. RESULTS AT 355 NM

The study at 355 nm was conducted only on the sputtered Al dots. Since the damage was much more severe at 355 nm than at 1064 nm, attention was focused on catastrophic damage (i.e. drilling or cracking of the window) and measurements of damage size were not performed. Damage stability maps were constructed to show the dependence of the onset of catastrophic damage on the fluence level and particle size (see Figs. 9 and 10).

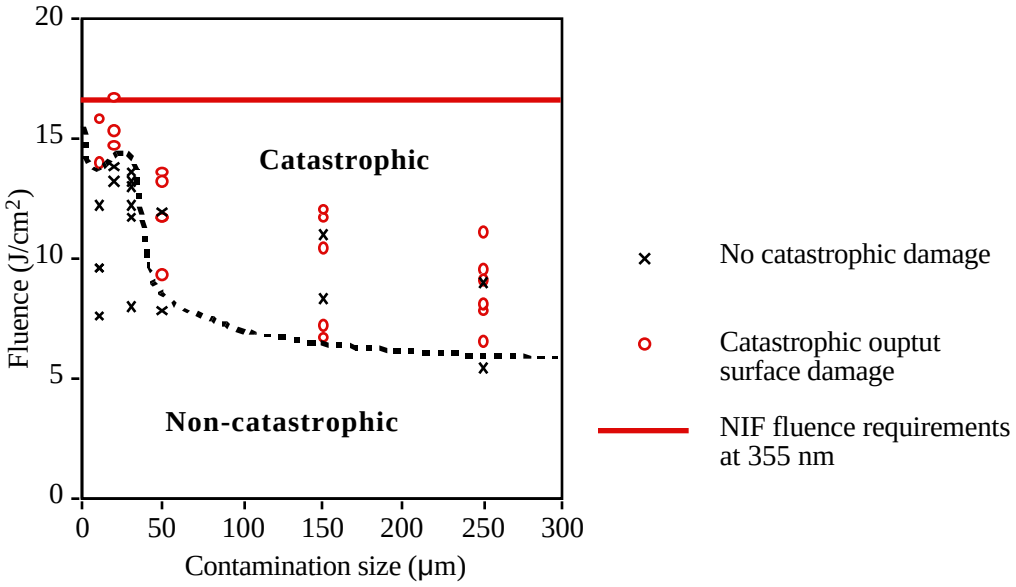

Fig. 9: Damage stability map at 355 nm showing the dependence of the onset of catastrophic damage on the fluence level and particle size for 1 μm thick sputtered Al dots located on the *input* surface of the silica window. The catastrophic damage was located on the output surface.

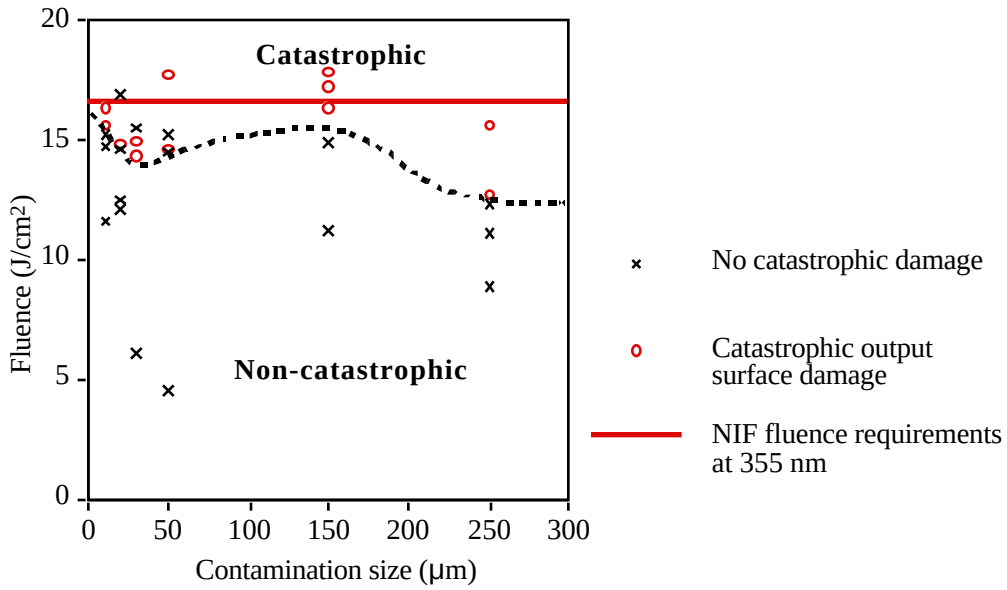

Fig. 10: Damage stability map at 355 nm showing the dependence of the onset of catastrophic damage on the fluence level and contaminant size for 1 μm thick sputtered Al dots located on the *output* surface of the silica window. The catastrophic damage was located on the output surface.

Both input and output surface contamination were found to have the potential for inducing catastrophic failure of the output surface of the glass at fluences as low as 6 J/cm^2 for the larger particles. Surprisingly, it was determined that input surface contamination had more negative effects than output surface contamination. The damage morphologies were very reproducible. Typical examples are shown in Figs. 11 and 12 for input and output contamination respectively.

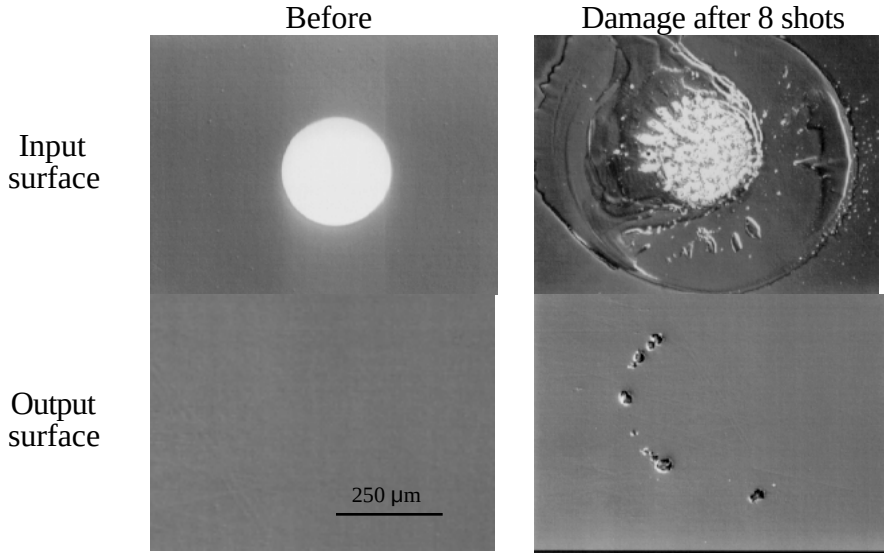

Fig. 11: Nomarski optical micrograph (from ref. 19) of the typical damage morphology of both input and output surfaces of the fused silica window after 8 shots on a 250 μm diameter, 1 μm thick Al dot, at 355 nm and 11 J/cm^2. The dot was located on the *input surface*.

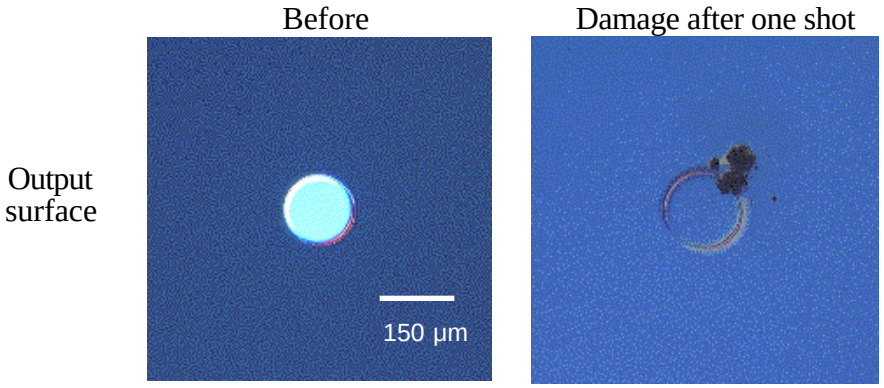

Fig. 12: Nomarski optical micrograph (from ref. 19) of the typical damage morphology of the output surface of the fused silica window after a single shot on a 150 µm diameter, 1 µm thick Al dot, at 355 nm and 15 J/cm^2. The dot was located on the *output surface*.

For input surface contamination, a plasma can ignite on the surface at fluences above 2 J/cm^2. A damage pattern with the shape of the particle on the input surface is often found on the output surface (see Figs. 11 and 13). The damage on the output surface was found to occur on the optical path of the beam and often grew catastrophically by drilling into the glass during repetitive illumination. The experimental results for other materials (i.e. Cu, TiO_2 and ZrO_2) and the modeling of damage initiation have been reported elsewhere.[19-20]

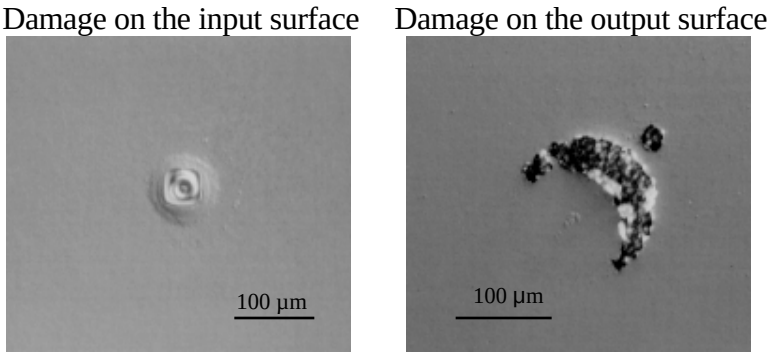

Fig. 13: Nomarski optical micrograph of damage after 2 shots at 355 nm and 15.8 J/cm^2 showing that the shape of the 20 µm contamination particle located on the input surface is often "printed" on the output surface.

5. CONCLUSIONS

The initial attempts to quantify the effects of contamination on laser-induced damage of fused silica optics are presented for Al particles located on input or output surfaces. The study was performed at 1064 and 355 nm and used an artificial method to contaminate optics which allowed rapid collection of large amounts of reproducible damage information.

The results show that a plasma can ignite at the contamination particle during shots at fluences above 2 J/cm^2. At 1064 nm, input surface contamination tends to splatter during repetitive illumination, leaving a burnt surface with a large number of small craters. The output surface occasionally fails catastrophically for large output surface shavings and high fluences. Output surface contaminants are usually ablated during the first shot, often leaving a fine wave pattern on the surface. The damage does not grow during subsequent shots unless the glass is cracked during the first shot. For 1 µm thick dots, the damage

size of particles less than 300 μm in diameter after 600 shots scales with the contaminant size. For these thin dots, the contamination size to damage size ratio equals on average 2.9 and 1.4 for input and output surface contamination, respectively.

At 355 nm, both input and output surface contaminants can initiate catastrophic failure of the output surface at relatively low fluences (6 J/cm^2 for 250 μm dots). Input surface contamination tends to have a more negative influence on the optics survivability.

These experimental observations show that contamination must be avoided on high power lasers. On-going work will be reported in the future to quantify the effects of the nature of the contamination material (metal, oxide, organics) and the substrate material.

6. ACKNOWLEDGMENTS

This work was performed under the auspices of the U.S. Department of Energy by Lawrence Livermore National Laboratory under Contract W-7405-Eng-48. The authors wish to acknowledge Lan Nguyen and Craig Alford for their participation in producing the silicon nitride membrane masks and the metal deposits.

7. REFERENCES

1. I. A. Fersman, L. D. Khazov, "The effect of surface cleanliness of optical elements on their radiation resistance", *Soviet Journal of Optical Technology* **37**, 627 (1971).

2. G. R. Wirtenson, "High fluence effects on optics in the Argus and Shiva laser chains", *Optical Engineering* **18**, 574 (1979).

3. B. E. Newnam, "Optical materials for high-power lasers: recent achievements", *Laser Focus* **18**, 53 (1992).

4. J. B. Heaney, H. Herzig, J. F. Osantowski, "Auger spectroscopic examination of MgF_2-coated Al mirrors before and after UV irradiation", *Applied Optics* **16**, 1886 (1977).

5. S. Guch, Jr. and F. E. Hovis, "Beyond perfection: The need for understanding contamination effects on real-world optics", *Laser-Induced Damage in Optical Materials, SPIE* **2114**, 505 (1994).

6. M. A. Acharekar, " Infra-red absorption spectroscopy of Nd:YAG and Nd:GSGG surface contaminants", *Laser-Induced Damage in Optical Materials, NBS SP* **746**, 170 (1985).

7. K. Mann, B. Wolff-Rottke, and F. Müller, "Removal of dust particles from metal mirror surfaces by eximer laser radiation", *Laser-Induced Damage in Optical Materials, SPIE* **2428**, 226 (1994).

8. D. Jollay, "Manufacturing experience in reducing environmental induced failures of laser diodes", *Laser-Induced Damage in Optical Materials, SPIE* **2714**, 679 (1995).

9. C. E. Geosling, "Clean cavity contamination in gas lasers", *SPIE* **2714**, 689 (1995).

10. G. A. Harvey, T. H. Chyba, and M. C. Cimolino, "Cleanliness and damage measurements of optics in atmospheric sensing high energy lasers", *Laser-Induced Damage in Optical Materials, SPIE* **2714**, 696 (1995).

11. F. E. Hovis, B. A. Sherperd, C. T. Radcliffe, A. L. Bailey, and W. T. Boswell, "Optical damage at the part per million level: The role of trace contamination in laser induced optical damage", *Laser-Induced Damage in Optical Materials, SPIE* **2428**, 72 (1994).

12. F. E. Hovis, B. Sherperd, C. T. Radcliffe, and H. A. Maliborski, "Mechanisms of contamination induced optical damage in lasers", *Laser-Induced Damage in Optical Materials, SPIE* **2428**, 72 (1994).

13. F. E. Hovis, B. A. Sherperd, C. T. Radcliffe, and H. A. Maliborski, "Contamination damage in pulse 1 μm lasers", *Laser-Induced Damage in Optical Materials, SPIE* **2714**, 707 (1995).

14. R. P. Gonzales and D. Milam, "Evolution during multiple-shot irradiation of damage surrounding isolated platinum inclusions in phosphate laser glasses", *Laser-Induced Damage in Optical Materials, NBS SP* **746**, 128 (1985).

15. M. R. Kozlowski, R. Chow, and I. M. Thomas, "Optical coatings for high power laser applications", Handbook of Laser Science and Technology, Supplement 2: Optical Materials, ed. M. J. Weber, CRC Press, 767, (1995).

16. M. D. Miller, R. Chow, and G. E. Loomis, "Electrostatic reduction of particulates for laser-resistant hafnia coatings", *Laser-Induced Damage in Optical Materials, SPIE* **2114**, 426 (1993).

17. J. T. Hunt, K. R. Manes, and P. A. Renard, "Hot images from obscurations", *Appl. Optics* **32**, 5973 (1993).

18. A. J. Morgan, F. Rainer, F. P. DeMarco, R. P. Gonzales, M. R. Kozlowski, and M. C. Staggs, "Expanded damage test facilities at LLNL", *Laser-Induced Damage in Optical Materials, NIST SP* **801**, 47 (1989).

19. F. Y. Génin, M. R. Kozlowski, and R. Brusasco, "Catastrophic failure of contaminated fused silica optics at 355 nm", *Solid State Lasers for Application to Inertial Confinement Fusion,* Paris, France, in press (1996)

20. M. D. Feit, A. M. Rubenchik, D. R. Faux, R. A. Riddle, A. Shapiro, D. C. Eder, B. M. Penetrante, D. Milam, F. Y. Génin, and M. R. Kozlowski, "Modeling of laser damage initiated by surface contamination", in these proceedings.